HAL
open science

Epigenetic status of H19/IGF2 and SNRPN imprinted genes in aborted and successfully derived embryonic stem cell lines in non-human primates

Florence Wianny, Thierry Blachère, Murielle Godet, Rémi Guillermas, Véronique Cortay, Pierre-Yves Bourillot, Annick Lefèvre, Pierre Savatier, Colette Dehay

To cite this version:

Florence Wianny, Thierry Blachère, Murielle Godet, Rémi Guillermas, Véronique Cortay, et al.. Epigenetic status of H19/IGF2 and SNRPN imprinted genes in aborted and successfully derived embryonic stem cell lines in non-human primates. Stem Cell Research, 2016, 16 (3), pp.557-567. 10.1016/j.scr.2016.03.002 . hal-02635946

HAL Id: hal-02635946

https://hal.inrae.fr/hal-02635946

Submitted on 27 May 2020

HAL is a multi-disciplinary open access archive for the deposit and dissemination of scientific research documents, whether they are published or not. The documents may come from teaching and research institutions in France or abroad, or from public or private research centers.

L'archive ouverte pluridisciplinaire **HAL**, est destinée au dépôt et à la diffusion de documents scientifiques de niveau recherche, publiés ou non, émanant des établissements d'enseignement et de recherche français ou étrangers, des laboratoires publics ou privés.

Distributed under a Creative Commons Attribution - NonCommercial - NoDerivatives 4.0 International License

Stem Cell Research 16 (2016) 557–567

Contents lists available at ScienceDirect

Stem Cell Research

journal homepage: www.elsevier.com/locate/scr

Epigenetic status of *H19/IGF2* and *SNRPN* imprinted genes in aborted and successfully derived embryonic stem cell lines in non-human primates

Florence Wianny [a,b,*], Thierry Blachère [a,b,1], Murielle Godet [a,b,c,1], Rémi Guillermas [a,b], Véronique Cortay [a,b], Pierre-Yves Bourillot [a,b], Annick Lefèvre [a,b], Pierre Savatier [a,b,2], Colette Dehay [a,b,2]

[a] INSERM, U1208, Stem Cell and Brain Research Institute, 18 Avenue Doyen Lépine, 69500 Bron, France
[b] Université de Lyon, Université Lyon 1, Lyon, France
[c] INRA, USC 1361, 69500 Bron, France

ARTICLE INFO

Article history:
Received 24 September 2015
Received in revised form 4 March 2016
Accepted 7 March 2016
Available online 9 March 2016

Keywords:
Embryonic stem cell
Non-human primate
Epigenetic
Imprinted genes
Methylation
H19/IGF2
SNRPN

ABSTRACT

The imprinted genes of primate embryonic stem cells (ESCs) often show altered DNA methylation. It is unknown whether these alterations emerge while deriving the ESCs. Here we studied the methylation patterns of two differentially methylated regions (DMRs), *SNRPN* and *H19/IGF2* DMRs, during the derivation of monkey ESCs. We show that the *SNRPN* DMR is characteristically methylated at maternal alleles, whereas the *H19/IGF2* DMR is globally highly methylated, with unusual methylation on the maternal alleles. These methylation patterns remain stable from the early stages of ESC derivation to late passages of monkey ESCs and following differentiation. Importantly, the methylation status of *H19/IGF2* DMR and the expression levels of *IGF2*, *H19*, and *DNMT3B* mRNAs in early embryo-derived cells were correlated with their capacity to generate genuine ESC lines. Thus, we propose that these markers could be useful to predict the outcomes of establishing an ESC line in primates.
© 2016 The Authors. Published by Elsevier B.V. This is an open access article under the CC BY-NC-ND license (http://creativecommons.org/licenses/by-nc-nd/4.0/).

1. Introduction

Genomic imprinting is an epigenetic mechanism that ensures the differential expression of imprinted genes in a parent-of-origin fashion. The alleles of imprinted genes are marked with their parental origin by DNA methylation at differentially methylated regions (DMRs), which are CpG-rich-cis-elements within the locus (Reik and Walter, 2001). In order to be inherited from one generation to the next, these epigenetic marks are erased early in life in primordial germ cells and reset in the germline as per sex (Hajkova et al., 2002). The altered methylation of imprinted genes leads to improper gene dosage during embryonic development and has been associated with several pathologies, including cancers and neurological disorders (Reed and Leff, 1994; Orstavik, 1999; Feinberg, 2004; Demars and Gicquel, 2012; Brioude et al., 2013; McCann et al., 1996; Takai et al., 2001). Recent studies have suggested that assisted reproductive technologies (ARTs), such as superovulation, *in vitro* fertilisation and embryo culture, favour acquisition of imprinting errors, which can lead to diseases and developmental defects (DeBaun et al., 2003; Gicquel et al., 2003; Maher et al., 2003; Orstavik et al., 2003; Borghol et al., 2006; Bowdin et al., 2007; Khoueiry et al., 2008; Grace and Sinclair, 2009; Chen et al., 2010; Ibala-Romdhane et al., 2011; Khoueiry et al., 2013). During the early stages of embryonic stem cells (ESCs) isolation from pre-implantation stage embryos, embryonic cells are subject to intense *in vitro* manipulation and environmental changes that may impact the epigenetic status and irreversibly alter the capacity to generate ESC lines or to exhibit the full differentiation potential of genuine ESCs. Primate ESCs often show altered DNA methylation on imprinted genes, particularly imprinted genes, such as *H19/insulin-like growth factor2* (*IGF2*) (Fujimoto et al., 2006; Mitalipov, 2006; Mitalipov et al., 2007; Frost et al., 2011). However, it is unknown whether these alterations emerge during ESC isolation and whether they are correlated with the ESC outcome. To address these questions, we analysed the methylation profiles of two well-characterised DMRs, *H19/IGF2* and *SNRPN* DMRs, while deriving monkey ESCs. The *H19/IGF2* DMR is the best candidate for this study because its methylation status is particularly sensitive to changes in culture conditions and differentiation (Sasaki et al., 1995; Doherty et al., 2000; Khosla et al., 2001; Mann et al., 2004). The *H19/IGF2* DMR acquires methylation in the paternal germline and is characteristically unmethylated on maternal alleles. The *H19/IGF2* DMR regulates the expression of two oppositely imprinted genes, such as *IGF2* and *H19*. The *IGF2* locus encodes *IGF2*, an autocrine/paracrine mitogen, and transcription of *H19* produces a

Abbreviations: ESC, embryonic stem cell; DMR, differentially methylated region; IGF, Insulin-like growth factor 2.

* Corresponding author.
E-mail address: florence.wianny@inserm.fr (F. Wianny).
[1] These authors contributed equally to this study.
[2] Co-senior authors.

http://dx.doi.org/10.1016/j.scr.2016.03.002
1873-5061/© 2016 The Authors. Published by Elsevier B.V. This is an open access article under the CC BY-NC-ND license (http://creativecommons.org/licenses/by-nc-nd/4.0/).

non-coding RNA, which is a precursor of a microRNA called miR-675 that negatively affects cell proliferation (Keniry et al., 2012). Hyper-methylation of this DMR can result in *IGF2* overexpression and is linked to an increased frequency of Beckwith–Wiedemann syndrome (DeBaun et al., 2003; Weksberg et al., 2003), whereas hypo-methylation of the paternal allele is associated with the Silver–Russell syndrome, which is characterised by slow growth before and after birth (Gicquel et al., 2005). In contrast to the *H19/IGF2* DMR, the *SNRPN* DMR is methylated on the maternal allele and unmethylated on the paternal allele. In humans, it is located on chromosome 15q11–13, which is a region involved in Prader–Willi and Angelman syndromes (AS) (Reed and Leff, 1994; Leff et al., 1992; Buiting et al., 1995). Methylation of this DMR is not sensitive to environmental alterations, including the *in vitro* manipulation of mouse ESCs (Schumacher and Doerfler, 2004), which makes it a good marker of methylation stability.

Here, we demonstrate that the methylation patterns of the *H19/IGF2* and *SNRPN* DMRs were stable from the early stages of derivation to late passages of monkey ESCs, and following *in vitro* differentiation. We also showed that the *H19/IGF2* DMR methylation pattern was correlated with the capacity of early embryo-derived cell lines to generate a *bona fide* ESC line.

2. Results

2.1. The SNRPN and H19/IGF2 DMR methylation patterns in the rhesus monkey ESC lines

First, we studied the epigenetic status of the rhesus monkey LYON-ES1 line (Wianny et al., 2008) during derivation and after long-term culture. We analysed *H19/IGF2* and *SNRPN* DMR methylation status using a sensitive bisulphite sequencing technique that previously enabled to perform a methylation analysis on single oocytes and early human embryos (Khoueiry et al., 2008; Lefevre and Blachere, 2015). Identification of single nucleotide polymorphisms (SNPs) within each DMR enabled allele-specific methylation analyses of parentally imprinted DMRs. The *SNRPN* DMR is classically methylated on the maternal allele and unmethylated on the paternal allele (Reed and Leff, 1994). We defined a SNP within the *SNRPN* DMR (a C/G polymorphism at position 126776; NC_007864.1) of the rhesus monkey genome to analyse the levels of *SNRPN* DMR methylation on the paternal and maternal alleles (Fig. 1A). We analysed 26 CpG sites within the DMR of each allele. At early stage of LYON-ES1 cell derivation (passage 7), the *SNRPN* DMR was differentially methylated, with a high level of methylation on the maternal allele (91.6%) and a low level of methylation on the paternal

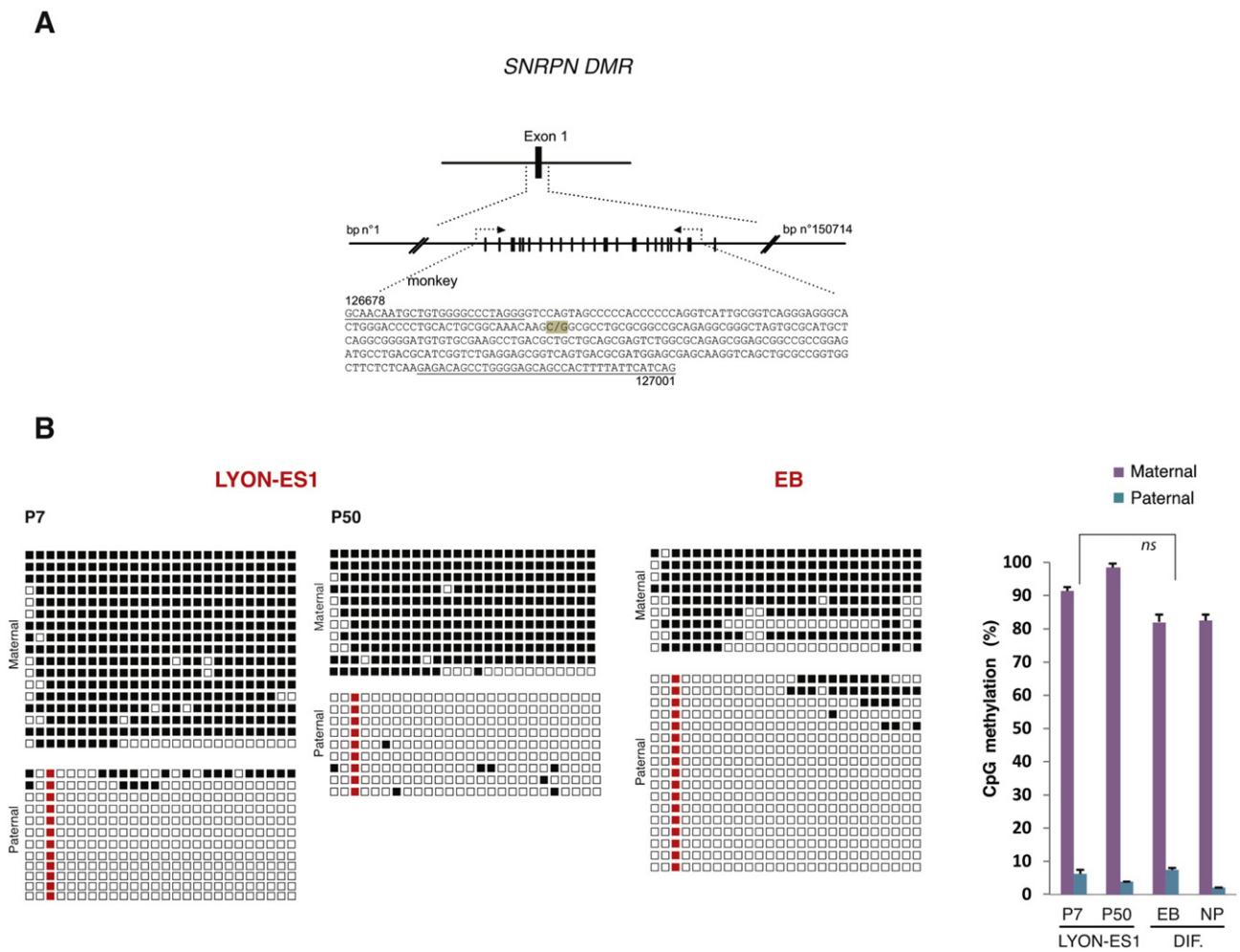

Fig. 1. Methylation status of the *SNRPN* differentially methylated region (DMR) in LYON-ES1 cells at early and late passages and after differentiation. A. Schematic representation of the *Macaca mulatta SNRPN* DMR. A 323 bp fragment of the *SNRPN* DMR (126678–127001, NC_007864.1) harbouring a single nucleotide polymorphism (SNP) G/C at nucleotide 126776 is shown. **B.** Left panel, bisulphite-sequencing analysis of the *SNRPN* DMR in LYON-ES1 cells at passages 7 and 50 and in EBs after 14 days of suspension culture. Each line represents a single allele. Black squares indicate methylated CpGs. White squares indicate unmethylated CpGs. Red squares indicate the SNP. Right panel, percentage of methylation of the *SNRPN* DMR in the maternal and paternal alleles of LYON-ES1 cells at passages 7 and 50 and after differentiation into EBs and NP after 40 days in culture. Mean ± standard error of the mean. Fisher's exact test was used to compute allele methylation status (ns, $p > 0.05$). DIF, differentiation; EB, embryoid bodies; NP, neural precursors; ns, not significant.

allele (6.3%) (Fig. 1B). Importantly, the *SNRPN* DMR exhibited the same methylation pattern at passage 50 (91.3% and 3.6% on the maternal and paternal alleles, respectively) (Fig. 1B), indicating that this pattern is stable over time in culture. Similar results were obtained for ORMES-1 and ORMES-6, two other rhesus ESC lines (Supplementary Fig. 1A). These results agree with published data for other monkey ESC lines (Mitalipov et al., 2007).

The *H19*/*IGF2* DMR is classically methylated on the paternal allele and unmethylated on the maternal allele (Zhang et al., 1993). We defined T/A at position 252 as an SNP in the CTCF-binding site of the *H19*/*IGF2* DMR (AY725988.1) to distinguish the parental origin of the alleles (Fig. 2A). At early stage of LYON-ES1 cell derivation (passage 7), the *H19*/*IGF2* DMR was highly methylated on the paternal allele (84%). In contrast, abnormal *H19*/*IGF2* DMR methylation was observed on the maternal allele (34%; Fig. 2B). The LYON-ES1 cells exhibited similar altered methylation pattern of *H19*/*IGF2* DMR at passages 33 and 50 (75% for the paternal allele; 28% and 24% for the maternal allele at passages 33 and 50, respectively) (Fig. 2B). Similar results were obtained for ORMES-1 and ORMES-6 cells, as well as for the human ESC line H9 (Supplementary Fig. 1B). Thus, the *SNRPN* and *H19*/*IGF2* DMR methylation patterns observed at the early stages of LYON-ES1 cell derivation were preserved during subsequent passages.

Next, we examined the *SNRPN* and *H19*/*IGF2* DMR methylation status during differentiation induced by growing monkey ESCs in suspension to generate embryoid bodies (EBs), which contain cells of the three germ lineages (Sasaki et al., 2005; Wianny et al., 2008). On day 14 of differentiation, the *SNRPN* DMR was still poorly methylated on the paternal allele (7.2%) but highly methylated on the maternal allele (82.7%) (Fig. 1B). The *H19*/*IGF2* DMR was highly methylated (66.2%) on the paternal allele and abnormally methylated (36.2%) on the

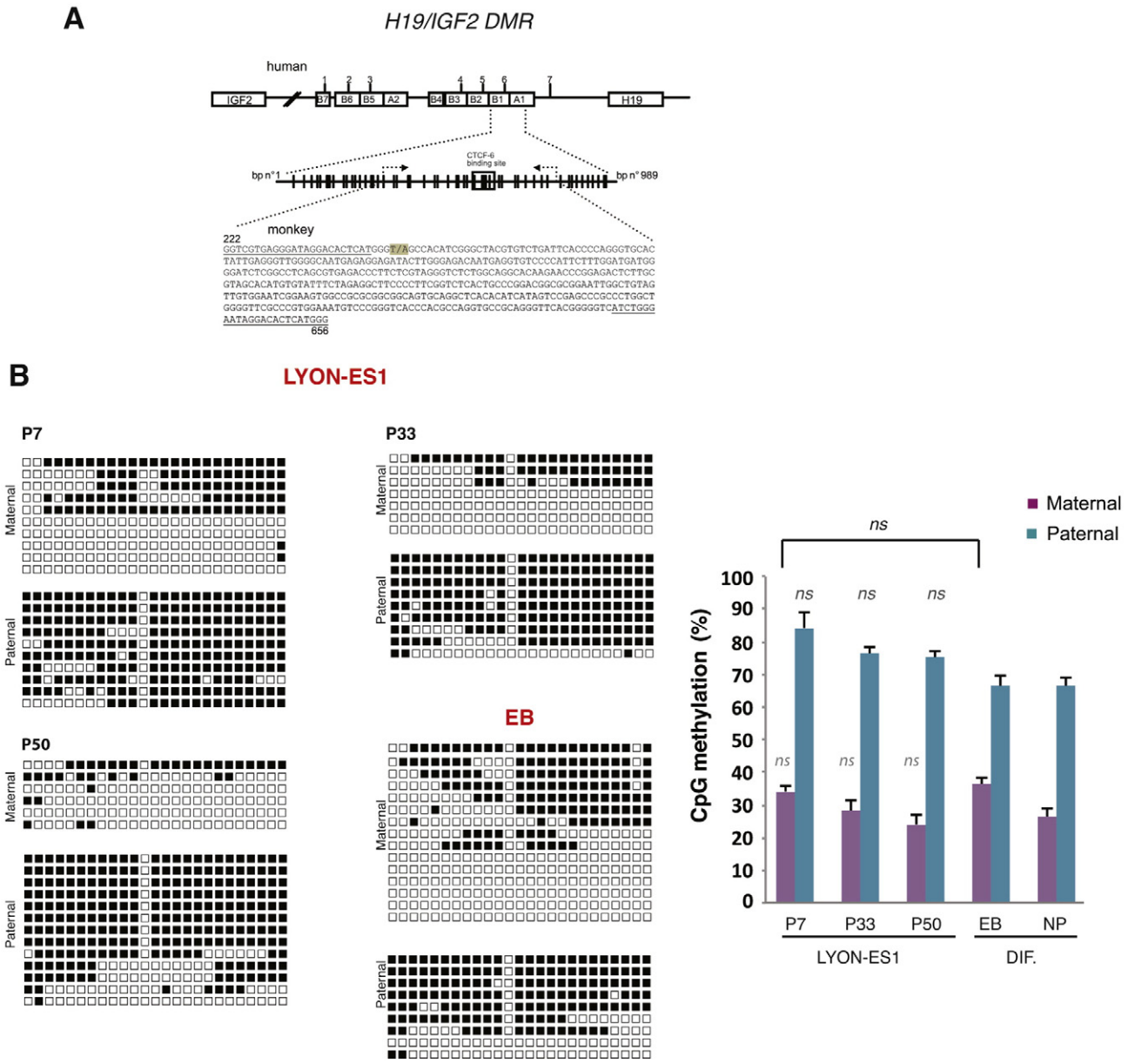

Fig. 2. Methylation status of the *H19*/*IGF2* differentially methylated region (DMR) in LYON-ES1 cells at early and late passages and after differentiation. A. Schematic representation of the *Macaca mulatta H19*/*IGF2* DMR. A 434 bp fragment of the *H19* DMR in the CTCF-binding site (222–656; AY725988.1) harbouring a single nucleotide polymorphism (SNP) T/A at nucleotide 249 is shown. **B.** Left panel, bisulphite-sequencing analysis of the *H19*/*IGF2* DMR in LYON-ES1 cells at passages 7, 33 and 50 and in EBs after 14 days of suspension culture (P5). Twenty to 40 clones were sequenced from each sample. Right panel, percentage methylation of the *H19*/*IGF2* DMR in maternal and paternal alleles of LYON-ES1 cells at passages 7, 33 and 50 and after differentiation into EBs and NP after 40 days in culture. Mean ± standard error of the mean. Fisher's exact test was used to compute allele methylation status (ns, $p > 0.05$). DIF, differentiation; EB, embryoid bodies; NP, neural precursors; ns, not significant.

maternal allele (Fig. 2B). Thus, the EBs exhibited similar *SNRPN* and *H19/IGF2* DMR methylation patterns as those of undifferentiated LYON-ES1 cells. Similarly, neural derivatives of LYON-ES1 cells propagated for 40 days exhibited *SNRPN* and *H19/IGF2* DMR methylation patterns similar to those described for undifferentiated LYON-ES1 cells (Figs. 1B and 2B).

Taken together, these results indicate that the LYON-ES1 cell line, exhibits a differential *SNRPN* DMR methylation pattern and aberrant *H19/IGF2* DMR methylation on the maternal allele, as observed in other primate ESC lines (Mitalipov et al., 2007; Nazor et al., 2012). They also suggest that these methylation patterns are highly stable during long-term self-renewal and differentiation.

2.2. SNRPN and H19/IGF2 DMR methylation patterns in pre-ESC lines

We generated 166 fertilised rhesus embryos following intracellular sperm injection (ICSI), of which thirty-four were developed to the blastocyst stage. Thirty embryos or inner cell masses (ICMs) attached to feeder cells, of which 15 produced an outgrowth that could be expanded for more than five passages. They include the LYON-ES1 cell line described above, and 14 lines, designated 19–33 (Sup. Table 1), that failed to expand beyond passage 20 and aborted during subsequent passages. These 14 lines are referred to as the pre-ESC lines.

LYON-ES1 cells showed a high proliferation rate (5.9 ± 0.9 days between two successive passages), similar to other monkey ESCs

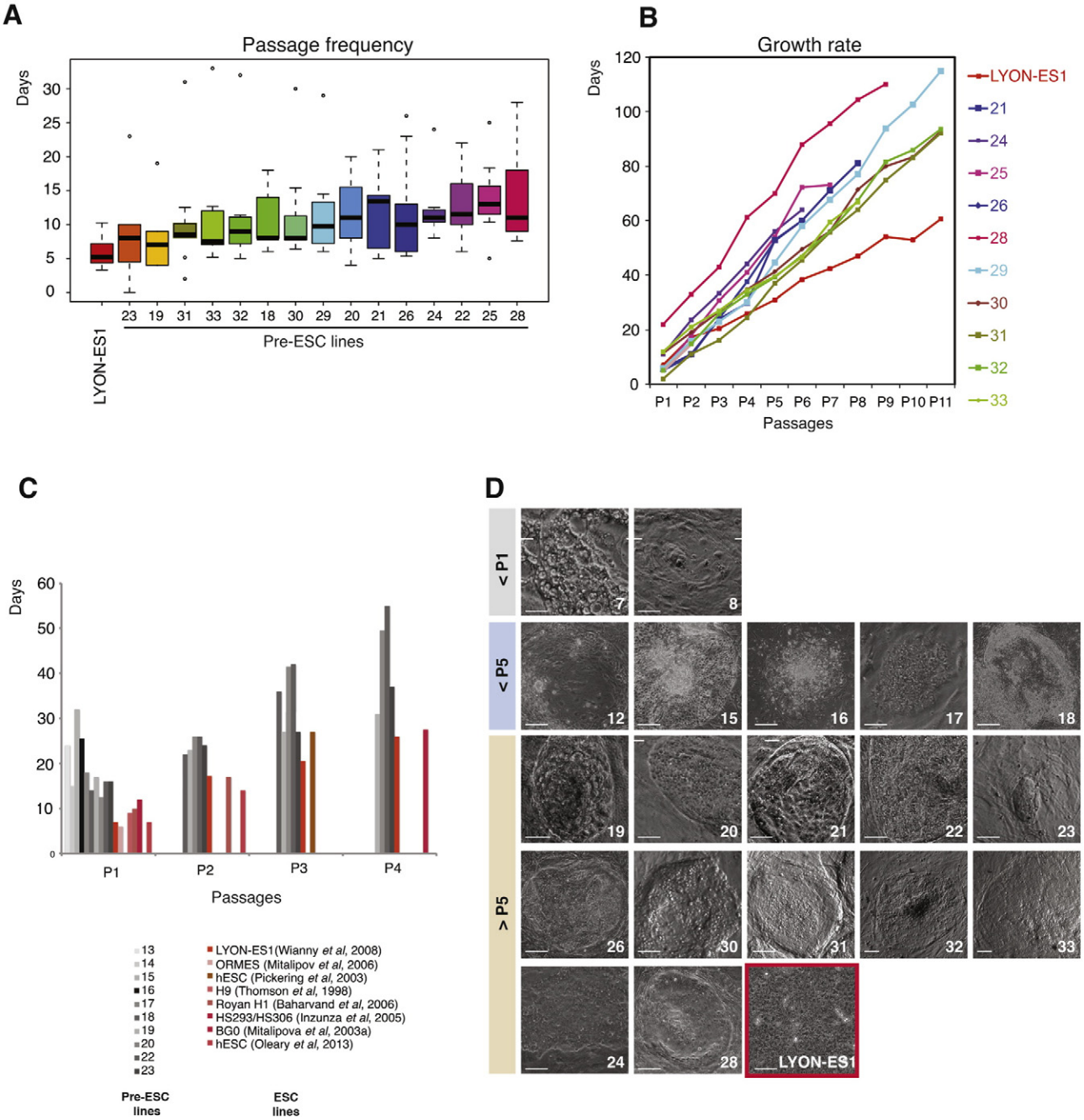

Fig. 3. Derivation of pre-ESC lines from early rhesus embryos. A. Box-and-whiskers plot representations of passage frequency (mean duration between two successive passages) for LYON-ES1 and the pre-ESC lines until passage 8. **B.** Growth rate of the pre-ESC lines and LYON-ES1 cell line until passage 11. Each line is represented with the same colour than in **A**. **C.** Data form the literature showing the growth rate of human and monkey ESC lines during the first five passages (compared to pre-ESC lines). **D.** Morphology and numbering of the cell lines according to the maximum number of passage reached *in vitro*. The LYON-ES1 cell line is indicated in red. The pre-ESC lines nb. 24 and 28 showed similar morphology to that of LYON-ES1 cell line. Scale bars, 100 μm.

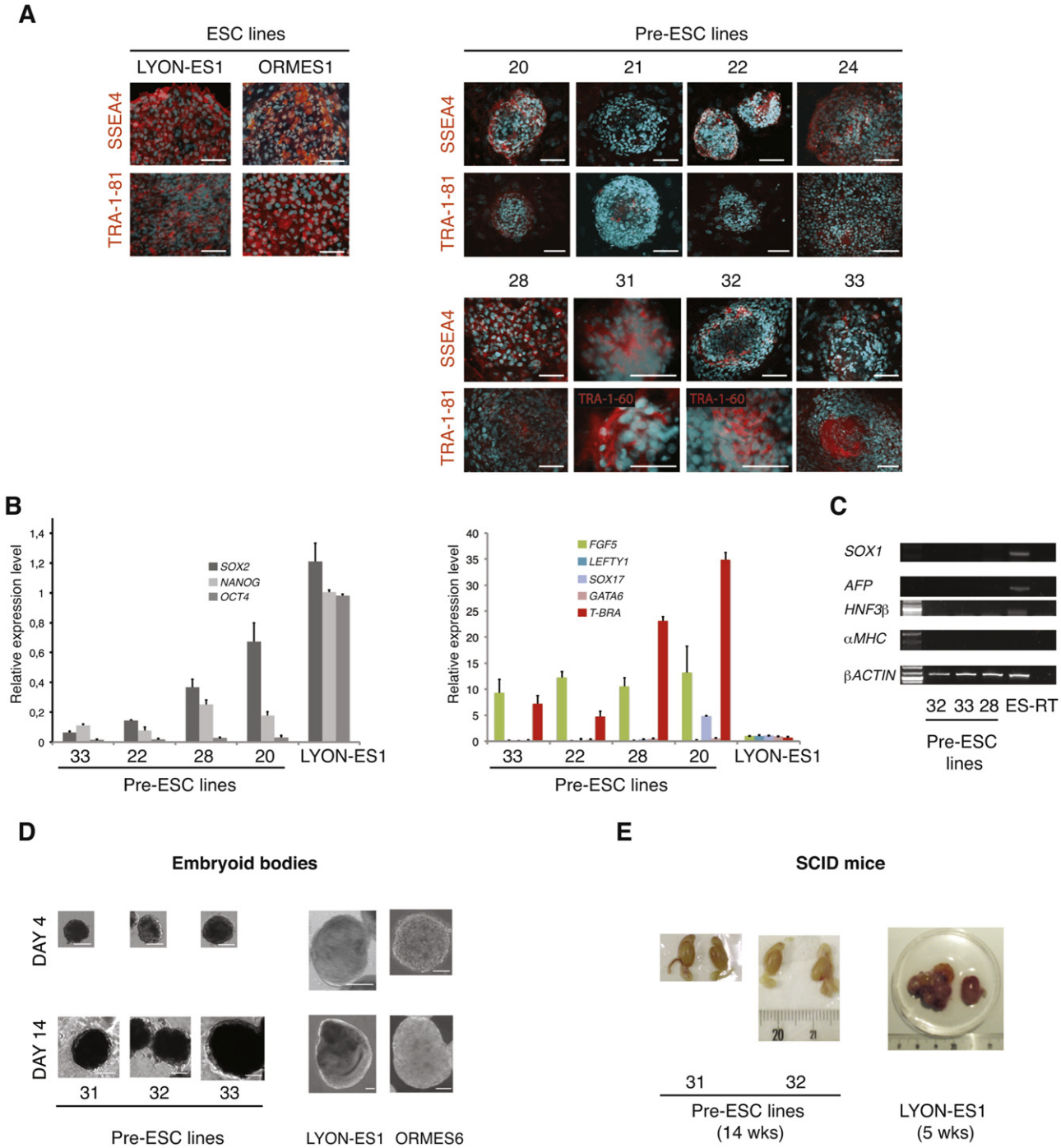

Fig. 4. Characterisation of the pre-ESC lines. A. Immunofluorescent staining for the SSEA4 and TRA-1-81 or TRA-1-60 surface antigens in rhesus monkey ESCs (LYON-ES1 and ORMES-1 lines) and the pre-ESC lines nb. 20, 21, 22, 24, 28, 31, 32 and 33. Nuclei were counterstained with Hoechst 33258 (blue). Scale bar, 100 μm. **B.** Levels of *SOX2*, *NANOG*, *OCT4* (left), *FGF5*, *LEFTY1 SOX17*, *GATA6* and *T-BRA* mRNAs measured by qPCR in the pre-ESC lines and LYON-ES (mean ± standard error of the mean calculated from three replicates after normalisation to *PGK1*). **C**. mRNA expression of the *SOX1*, *AFP*, *HNF-3β*, α-*MHC* differentiation markers measured by RT-PCR in the pre-ESC and LYON-ES1 cell lines (ES). **D.** Morphology of the EBs after 14 and 4 days of culture of pre-ESC lines 31, 32 and 33, LYON-ES1 and ORMES-6 cells. Scale bar, 200 μm. **E**. Teratoma formation 14 weeks after injecting pre-ESC lines 31 and 32 and 5 weeks after injecting LYON-ES1 cells in the testis of SCID mice. Two mice for each cell line were studied and produced similar results. AFP, alpha feto protein; FGF, fibroblast growth factor; HNF, hepatocyte nuclear factor; MHC, myosin heavy chain; wks, weeks.

(Fluckiger et al., 2006) and reached passage 10 in 53 days (Fig. 3A and B). In contrast, the pre-ESC lines exhibited a slower growth rate than other monkey and human ESC lines at early stages of derivation (Thomson et al., 1998; Mitalipova et al., 2003; Pickering et al., 2003; Inzunza et al., 2005; Baharvand et al., 2006; Mitalipov et al., 2006; O'Leary et al., 2013) (Fig. 3B and C), resulting in culture durations of 7.6–16 days between two successive passages (passage 10 was reached after 83–102 days, depending on the pre-ESC line). Most of the pre-ESC lines grew as three-dimensional compact colonies with poorly visible nuclei (Fig. 3D). Only two (lines 24 and 28) cell lines displayed typical monkey ESC morphology with a high nuclear/cytoplasmic ratio. No morphological changes were observed after long-term culture of these two lines (data not shown). Eight pre-ESC lines (Khoueiry et al., 2013; Fujimoto et al., 2006; Mitalipov, 2006; Frost et al., 2011; Mann et al., 2004) were expanded and analysed for the expression of cell surface markers. All of them expressed the SSEA4, TRA-1-60 and/or TRA-1-81

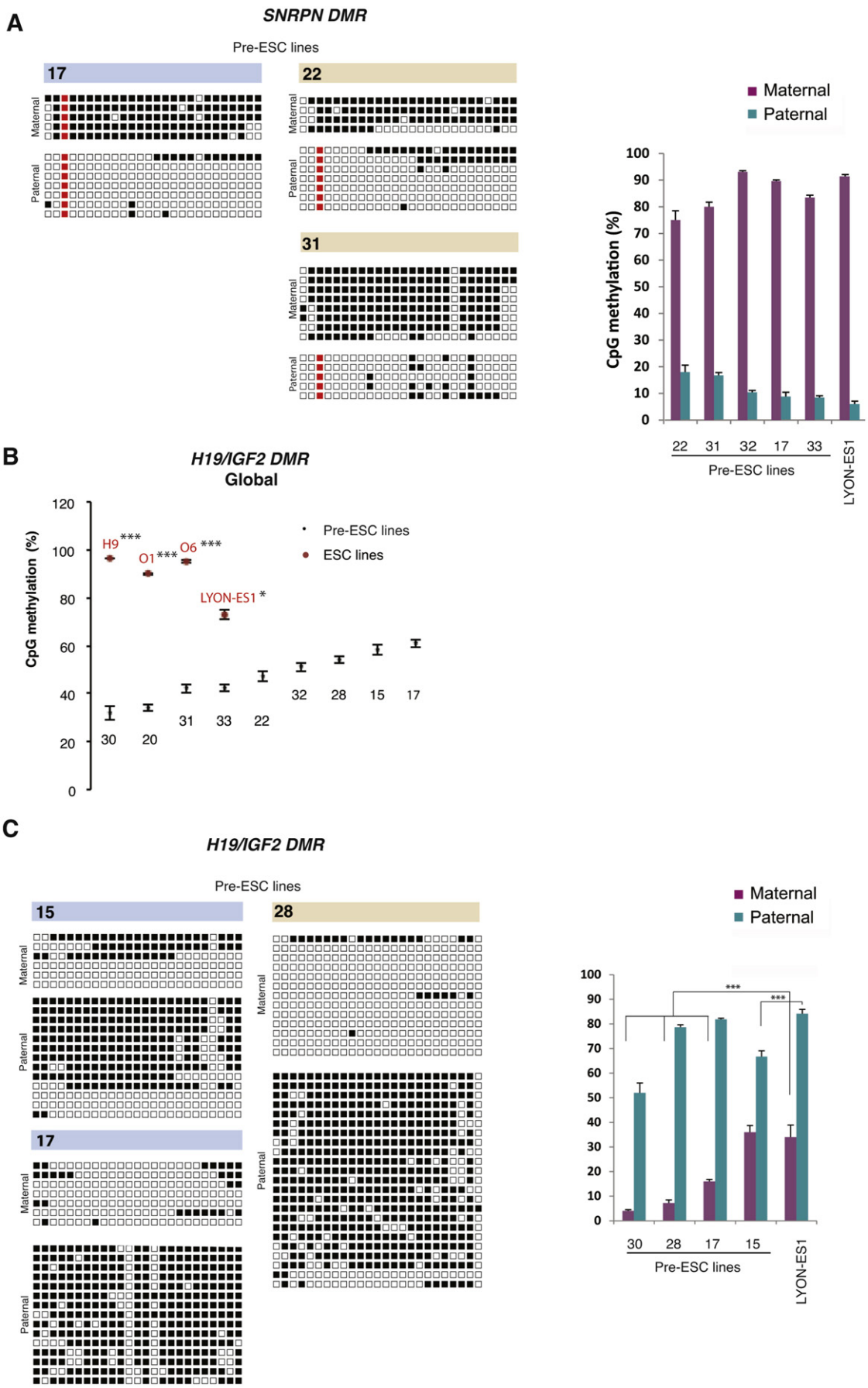
A
SNRPN DMR
Pre-ESC lines
17
22
31
Maternal
Paternal
Maternal
Paternal
CpG methylation (%)
22 31 32 17 33
Pre-ESC lines
LYON-ES1
B
H19/IGF2 DMR
Global
CpG methylation (%)
Pre-ESC lines
ESC lines
H9***
O1***
O6***
LYON-ES1 *
30 20 31 33 22 32 28 15 17
C
H19/IGF2 DMR
Pre-ESC lines
15
28
17
Maternal
Paternal
30 28 17 15
Pre-ESC lines
LYON-ES1

primate ESC surface markers (Fig. 4A). Some of the cell lines were positive for alkaline phosphatase (Supplementary Fig. 2). Extensive gene expression analysis of these slow growing pre-ESCs could not be performed; we thus analysed several pluripotent and differentiation markers using RT-PCR. We observed that pre-ESC lines 20, 22, 28 and 33 expressed the *OCT4*, *SOX2* and *NANOG* pluripotency markers, albeit at lower levels than those expressed by LYON-ES1 cells (Fig. 4B). Some pre-ESC lines also expressed the early lineage markers associated with primed pluripotency, such as *T-BRA*, *FGF5* and *SOX17* (Joo et al., 2014; Chen et al., 2015) (Fig. 4B), at a much higher level than genuine ESCs. Similar to LYON-ES1 cells, the pre-ESC lines did not express the late differentiation markers *SOX1*, *AFP*, *HNF-3β* or *α-MHC* (Fig. 4C). These results suggest that the pre-ESC lines displayed features of primate ESCs, but were engaged into early differentiation. After a 7-day culture in the absence of feeder cells, the morphology of the pre-ESC lines became heterogeneous and *OCT4* and *NANOG* expression decreased (Supplementary Fig. 3A and B), indicating differentiation. Pre-ESC lines 31–33 produced small-size EBs in suspension culture and displayed low growth rates, as judged by limited increases in EB size after 2 weeks *in vitro* (Fig. 4D). In contrast, LYON-ES1 cells produced fully developed EBs after 4 days of culture with the rapid expansion of size over time (Fig. 4D). Moreover, differentiation markers for the three germ lineages were expressed (Wianny et al., 2008). In addition, the pre-ESC lines (nb. 31, 32) failed to produce teratomas after 14 weeks when injected into the testis of immunocompromised mice. In contrast, LYON-ES1 cells injected under the same conditions produced teratomas after 5 weeks (Fig. 4E).

Thus, the pre-ESC lines can be defined as embryo-derived cell lines that failed to expand beyond passage 20. They displayed an impaired capacity to self-renew and to differentiate *in vitro* and *in vivo*.

Next, we investigated methylation status of the *SNRPN* and *H19* DMRs in several pre-ESC lines. The *SNRPN* DMR analysed among the five pre-ESC lines was weakly methylated on the paternal allele (0.8–18%) but highly methylated on the maternal allele (74–93%), which was similar to the results observed in LYON-ES1 cells (Fig. 5A). This finding suggests that methylation of the *SNRPN* DMR does not differ between the *bona fide* and pre-ESC lines. In contrast, the global methylation rate of the *H19/IGF2* DMR varied and was always lower in the pre-ESC lines (range, 32–61% in the nine lines analysed) than that in the *bona fide* ESC lines (73% in LYON-ES1 cells, $p < 0.05$; 90%, 95% and 96%, in ORMES-1, ORMES-6 and human H9 ESCs, respectively, $p < 0.001$) (Fig. 5B). We took advantage of SNP found in the *H19/IGF2* DMR CTCF-binding site to determine the parental origin of the alleles in four of the nine pre-ESC lines analysed (nb. 15, 17, 28 and 30; Fig. 5C). In three of four pre-ESC lines (nb. 17, 28 and 30), the *H19/IGF2* DMR methylation rate on the maternal alleles was significantly lower (mean, 9%) than that in the *bona fide* ESC lines at early passage (34%) (Fig. 5C). In the fourth line (nb. 15), the *H19/IGF2* DMR methylation rate on the paternal allele was significantly lower (67%) than that in LYON-ES1 cells (84%). Taken together, these findings suggest that the *H19/IGF2* DMR methylation pattern distinguishes *bona fide* ESC lines from pre-ESC lines.

2.3. H19, IGF2 and DNMT3B mRNA levels characterise bona fide primate ESCs

Methylation of DMRs is typically linked to gene repression. Thus, we were interested in determining whether the differences observed in *H19/IGF2* DMR methylation were associated with altered *IGF2* or *H19* mRNA expression levels. We found that *H19* and *IGF2* were expressed during the early stage of LYON-ES1 cell derivation (passage 3) but the level of expression sharply decreased at later passages (passages 16 and 43) in LYON-ES1 cells, as observed in other monkey ESC lines ORMES1, ORMES6 and human ESC lines H1, H9 and HS306 (Fig. 6A). In contrast, all pre-ESC lines expressed lower levels of *NANOG* and failed to downregulate *H19* and *IGF2* expression, as indicated by high levels of expression (Fig. 6A).

We next assessed the expression of *DNA methyltransferases* (*DNMT*)*1*, *3A* and *3B*, which are responsible for the establishment and maintenance of embryonic methylation patterns (Okano et al., 1999; Watanabe et al., 2002). *DNMT1*, *DNMT3A* and *DNMT3B* were expressed at early stages of LYON-ES1 derivation and remained highly expressed in LYON-ES1 cells and in all primate ESCs analysed (ORMES-1, ORMES-6, H1, H9 and HS306 cells) as previously shown (Tang et al., 2010; Sperger et al., 2003; Adewumi et al., 2007; Nissenbaum et al., 2013; Liao et al., 2015) (Fig. 6A). In contrast, all pre-ESC lines expressing pluripotency markers (nb. 20, 22, 28, 32 and 33) (Figs. 4A,B and 6A; Supplementary Table 2) expressed low levels of *DNMT3B* (Fig. 6B).

Overall, our results suggest that the *bona fide* ESC lines can be distinguished from pre-ESCs, by low expression levels of *H19* and *IGF2 mRNAs* and elevated expression level of *DNMT3B* mRNA. Most notably, *bona fide* ESCs exhibit a high degree of *H19/IGF2* DMR methylation, characterised by abnormal methylation on the maternal allele (mean, 28%). This specific methylation pattern was maintained in the ESC lines from the early stages of derivation to late passages and after differentiation.

3. Discussion

The early steps of deriving ESCs are crucial, as the cells are easily affected by changes in culture conditions and *in vitro* manipulation, which may alter the methylation status of the sensitive imprinted genes. We found that the *SNRPN* and *H19/IGF2* DMR methylation patterns observed at the early stages of monkey ESC line derivation did not vary after long-term expansion or differentiation *in vitro*. We showed that the LYON-ES1 cell line, exhibited an altered *H19/IGF2* DMR methylation pattern (high global methylation rate, with unusual methylation at maternal alleles), as described previously in other primate ESC lines (Mitalipov et al., 2007; Nazor et al., 2012). It is unknown whether this aberrant methylation pattern emerged in the oocyte during gametogenesis, following hormonal stimulation, or during embryonic development *in vitro*. We previously reported alterations in the *H19/IGF2* DMR methylation pattern in human oocytes following ART (Al-Khtib et al., 2011) and in human embryos produced by ICSI (Ibala-Romdhane et al., 2011; Khoueiry et al., 2013). A previous study reported that *H19* and *IGF2* are normally imprinted in ICSI produced monkey blastocysts produced by ICSI (Fujimoto et al., 2006). However, that study focused on the allele-specific *H19/IGF2* expression pattern and did not address *per se* the *H19/IFG2* DMR methylation status in embryos. There may be some discordance between DMR methylation and allelic expression in monkey embryos, as shown in human ESCs (Frost et al., 2011; Kim et al., 2007a; Grybek et al., 2014; Rugg-Gunn et al., 2005).

We found that the global methylation rate of the *H19/IGF2* DMR varied but was significantly lower in pre-ESCs than that in *bona fide* primate ESC lines. We hypothesised that differentiation began rapidly after plating the ICMs on feeder cells in some of pre-ESC lines

Fig. 5. Methylation status of the *SNRPN* and *H19/IGF2* differentially methylated regions (DMRs) in the pre-ESC linesA. Left panel, bisulphite-sequencing analysis of the *SNRPN* DMR in pre-ESC lines nb. 17, 22 and 31. Each line represents a single allele. Black squares indicate methylated CpGs. White squares represent unmethylated CpGs. Red square indicates the single nucleotide polymorphism (SNP) C/G. Right panel, percentage methylation of the *SNRPN* DMR in maternal and paternal alleles of the pre-ESC lines, compared with that in LYON-ES1 cells at passage 7. Mean ± standard error of the mean. **B.** Global methylation rate of the *H19/IGF2* DMR in the pre-ESC lines. Each pre-ESC line was compared to LYON-ES1 cell (passage 7), ORMES-1, ORMES-6 and the H9 human ESC lines. (ANOVA, * $p < 0.05$, *** $p < 0.001$). **C.** Left panel, bisulphite-sequencing analysis of the *H19/IGF2* DMR in pre-ESC lines nb. 15, 17 and 28; right panel, percentage methylation of the *H19/IGF2* DMR in the maternal and paternal alleles of the pre-ESC lines and LYON-ES1 cells at passage 7. Mean ± standard error of the mean. Fisher's exact test: *, $p < 0.05$; *** $p < 0.001$. Different colours associated with the numbering of the pre-ESC lines indicate the maximum passage reached by the line (blue, less than five passages; brown, more than five passages).

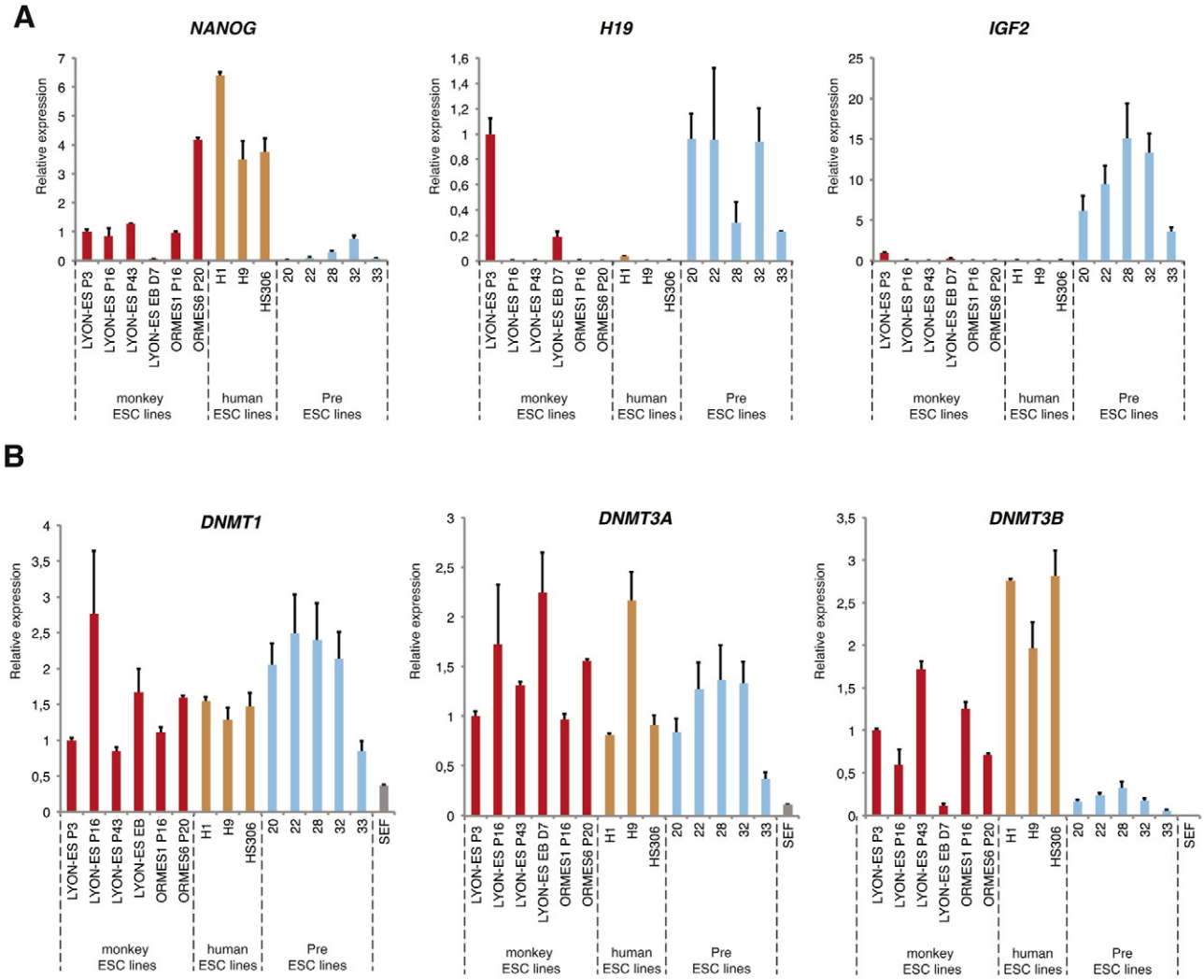

Fig. 6. *H19, IGF2, DNMT1, DNMT3A* and *DNMT3B* mRNA expression levels in the *genuine bona fide* ESC lines and pre-ESC lines (**A**) *NANOG*, *IGF2* and *H19* mRNA expression levels, and (**B**) *DNMT1*, *DNMT3A* and *DNMT3B* mRNA expression levels measured by qPCR in the monkey ESC lines: LYON-ES1 cells (passages 3, 16 and 43), LYON-ES1 cell-derived EBs (7 days), ORMES-1 cells (passage 16), ORMES-6 cells (passage 20); in the human ESC lines (H1; H9 and HS306); and in pre-ESC lines 20, 22, 28, 32, 33.

concomitant with a decrease in the *H19*/*IGF2* DMR methylation rate. Indeed, we showed that the pre-ESC lines did not exhibit all features of a *bona fide* ESC line. However, molecular characterisation of the pre-ESCs suggested that they retained some ESC features and that they contained cells only recently engaged in differentiation. More importantly, we showed that the *H19*/*IGF2* DMR methylation pattern remained stable after differentiation of LYON-ES1 cells into EBs and neural precursors. These results agree with previous studies reporting that epigenetic marks are stably inherited in differentiating human ESCs (Sun et al., 2006; Allegrucci et al., 2007). This finding supports the hypothesis that the *H19*/*IGF2* DMR methylation pattern observed in pre-ESCs (low methylation rate on maternal and/or paternal alleles) compared to that in the *bona fide* ESC lines and their differentiated derivatives was not merely a consequence of cell differentiation but rather due to the lack of acquiring or maintaining ESC properties.

In addition, our results also show that the expression level of *IGF2* and *H19* mRNA decreased during ESC isolation, from early to late passages of ESCs, in agreement with published human and mouse data (Sun et al., 2006; Humpherys et al., 2001; Rugg-Gunn et al., 2007; Mai et al., 2011; Sun et al., 2012). In contrast, the methylation rate of *H19*/*IGF2* DMR remained stable from early to late passages, highlighting discordance between methylation status and expression levels of *H19* and *IGF2* during derivation of monkey ESC lines. This observation may be surprising because *H19*/*IGF2* DMR is methylated on the paternal allele in monkey ESCs, and this is generally associated with the expression of *IGF2* and reciprocal silencing of *H19*. Some discordance between DMR methylation and allelic expression has previously been shown in mouse and human ESCs (Sun et al., 2012; Kim et al., 2007b). ESC lines are isolated from early embryos at a stage of intense epigenetic remodelling, and embryonic cells must quickly adapt to the *in vitro* culture environment. Modulation of the methylation rate at others sites than *H19*/*IGF2* DMR, as well as other epigenetic mechanisms such as histone modifications, may be involved in the modulation of expression of *H19* and *IGF2* during these processes. Furthermore, in the preimplantation stage mouse embryo, expression of *H19 and IGF2* is restricted to cells destined to colonise trophectoderm derivatives (Lee et al., 1990; Negron-Perez et al., 2013). Thus, we hypothesise that a fraction of differentiated cells that express high levels of *H19* and *IGF2* mRNAs are present during the early stages of ESC line derivation, and progressively lost after ESC selection and expansion.

In contrast to *bona fide* ESC lines, the pre-ESC lines expressed *H19* and *IGF2* mRNAs and lower levels *of DNMT3B*. This may reflect their limited ability to differentiate into the three germ layers, as a high *H19* expression level has been associated with altered differentiation potential in parthenogenetic ESCs (Ragina et al., 2012), and DNMT3B confers the capacity to form teratomas (Chen et al., 2003). This also suggests that

pre-ESCs failed to downregulate *H19* and *IGF2* expression, and that the epigenetic mechanisms involved in initiating self-renewal were not properly established or maintained in these cell lines.

Importantly, the high degree of methylation of the *H19/IGF2* DMR was not detrimental for maintaining pluripotent status of the monkey ESCs. Indeed, monkey ESC lines that exhibit such an 'altered' methylation profile are fully pluripotent (Fujimoto et al., 2006; Mitalipov et al., 2007) and show a normal karyotype after long-term culture (Wianny et al., 2008; Thomson et al., 1998; Mitalipov et al., 2006). Thus, rather than being considered as a deleterious criterion for the safety of ESC use in clinical research, a high degree of *H19/IGF2* DMR methylation might be a common signature of pluripotency in primates. An analysis of other paternally imprinted DMRs, such as the IG-DMR associated with pluripotency in mouse ESCs (Stadtfeld et al., 2010) will be required to determine whether this signature is restricted to the *H19/IGF2* locus.

We propose that the *H19/IGF2 DMR* methylation pattern and the expression levels of *H19*, *IGF2*, and *DNMT3B* mRNA could be used in conjunction with other well-known pluripotent markers to predict the outcome of ESC line isolation in monkeys.

4. Material and methods

4.1. Rhesus monkey embryo production using ICSI

Refer to our previous study for details about the embryo production and culture procedures (Wianny et al., 2008). All experiments were performed in compliance with national and European laws as well as with institutional guidelines concerning animal experimentation. Surgical procedures were performed in accordance with European requirements 2010/63/UE. All experimental procedures were designed with reference to the recommendations of the Weatherall report entitled 'The use of non-human primates in research.' Laboratory authorisation was provided by the 'Préfet de la Région Rhône-Alpes' and the 'Directeur départemental de la protection des populations' under permit no: #A690290402.

4.2. Isolation and culture of the embryonic cell lines

Methods for deriving embryonic cell lines from rhesus monkey embryos produced by ICSI have been described previously (Wianny et al., 2008). In brief, zonae pellucidae of pre-implantation stage embryos (16 cell/morula or blastocysts) were removed after brief exposure (45–60 s) to 0.5% pronase. Expanded blastocysts with distinct ICMs were subjected to immunosurgery. Isolated ICMs or whole embryos were plated onto Nunc 4-well dishes containing a feeder layer of mitomycin-C treated mouse embryonic fibroblasts (MEFs). Two culture media were used during the early stages of derivation (Supplementary Table 1): (1) knockout (KO)-DMEM medium containing 20% foetal bovine serum (FBS) supplemented with 1% non-essential amino acids (Invitrogen, Carlsbad, CA, USA), 2 mM L-glutamine (Invitrogen) and 0.1 mM β-mercaptoethanol and (2) KO-DMEM medium containing 10% FBS/10% Knockout Serum Replacement (KOSR; Invitrogen), supplemented with 4 ng/ml basic fibroblast growth factor (bFGF; Millipore Corp. Billerica, MA, USA), 1000 IU/ml human recombinant leukaemia inhibitory factor, 1% non-essential amino acids, 2 mM L-glutamine and 0.1 mM β-mercaptoethanol. ICMs or embryos that attached to the feeder layer and initiated outgrowth were dissociated manually into small cell clumps and re-plated on new MEFs. Emerging colonies were selected for further propagation, characterisation, epigenetic analysis and freezing. During the early stage of derivation, half of the medium was changed every other day. Passages were performed manually by cutting the colonies in big clumps using a flame-pulled Pasteur pipette. The colonies were re-plated on dishes with fresh feeder layers. Cultures were maintained at 37 °C in 5% CO_2. KO-DMEM medium containing 20% KOSR, supplemented with 4 ng/ml bFGF, 1% non-essential amino acids, 2 mM L-glutamine and 0.1 mM β-mercaptoethanol was used to maintain and amplify the monkey and human ESCs. EBs and neural precursors were obtained as described previously (Wianny et al., 2008).

4.3. Teratoma formation

Colonies of embryonic cells were inoculated beneath the testicular capsules of 7 week old severe combined immunodeficient (SCID) male mice (CB17/SCID; Charles River Laboratories, Shanghai, China; http://www.criver.com). The mice were euthanised, and the lesions were removed surgically 5–15 weeks later (LYON-ES1 cells and pre-ESC lines, respectively). Teratomas were fixed in 4% PFA overnight at 4 °C, incubated in 10% sucrose for 24 h, in 20% sucrose for 24 h and embedded in OCT embedding medium (CellPath, Newtown, UK; http://www.cellpath.co.uk). Cryosections (20 μm) were washed three times for 10 min in Tris-buffered saline (TBS) and processed for immunofluorescence staining (see (Wianny et al., 2008) for full analysis of teratomas).

4.4. Immunofluorescence

Cells were fixed in 2% PFA in phosphate-buffered saline (PBS) at 4 °C for 1 h and permeabilized in TBS + 0.1% Triton X-100 (three times for 10 min each). Non-specific binding was blocked with 10% normal goat serum or normal donkey serum (Jackson Immunoresearch Laboratories, West Grove, PA, USA; http://www.jacksonimuno.com) for 20 min at room temperature (RT). Cells were incubated overnight at 4 °C with primary antibodies (monoclonal anti-SSEA4; 1:100; MAB4304; monoclonal anti-TRA-1-60; MAB4360, 1:100; monoclonal anti-TRA-1-81, MAB4381, 1:100 Chemicon, Temecula, CA, USA: http://www.chemicon.com) diluted in diluent (Dako, Glostrup, Denmark; http://www.dako.fr). After three rinses in TBS, the cells were exposed to either affinity-purified goat or donkey anti-mouse, anti-rat, anti-rabbit or anti-goat immunoglobulin G or M conjugated either to Alexa488, 555 or 647 (Invitrogen) for 1 h at RT. Nuclei were counterstained with 1 mM 4′, 6-diamidino-2-phenylindole for 3 min. Coverslips were mounted on the slides after three rinses in TBS. The slides were examined by confocal microscopy under UV light to detect isothiocyanate (450–490 nm filter), indocarbocyanine 3 (550–570 nm filter) and Hoechst 33258 fluorescence (355–425 nm filter).

4.5. Semi-quantitative reverse transcription-polymerase chain reaction (RT-PCR)

Total RNA was prepared with a Qiagen RNeasy kit (Qiagen, Valencia, CA, USA; http://www.qiagen.com). Standard reverse transcription reactions were performed with 1 μg total RNA primed with random primers using the RevertAidH minus First strand cDNA synthesis kit (Biofidal, Vaulx En Velin, France; http://www.biofidal.fr). PCR was conducted with the PCR Master Mix (New England Biolabs, Ipswich, MA, USA; http://www.neb.com) using the following parameters: denaturation at 95 °C for 30 s, annealing at a suitable annealing temperature for 30 s and polymerisation at 72 °C for 30 s. The primer sequences and the number of cycles used are listed in Supplementary Table 3. An extension step of 7 min at 72 °C was added at the end of the cycles. Each PCR was performed under linear conditions. Reactions without reverse transcriptase were performed to control for genomic DNA contamination, using β-actin primers. PCR products were analysed on a 1.5% agarose gel and visualised with ethidium bromide.

4.6. Real-time qPCR

RNA was extracted using RNAeasy kits and on-column DNAse digestion. Reverse transcription was carried out with MuMLV-RT (Promega, Madison, WI, USA; http://www.promega.com), according to the manufacturer's recommendations. The primer sequences are listed in Supplementary Table 3. Quantitative PCR was performed using the qPCR system and Fast SYBR Green I Master Mix (Applied Biosystems,

Foster City, CA, USA), according to the manufacturer's instructions. All normalisations were carried out using PGK1.

4.7. DNA methylation analysis

The methylation profiles of the *H19/IGF2* DMR and the *SNRPN* DMR were determined by bisulphite mutagenesis and sequencing, as described previously (Lefevre and Blachere, 2015). DNA was extracted with the Nucleospin® Tissue kit for tissues (Macherey-Nalgel, Hoerdt, France). The EpiTect® Plus DNA Bisulfite Kit (Qiagen) was used according to the manufacturer's recommendations. The cells were directly incubated in the kit lysis buffer prior to bisulphite treatment. The bisulphite conversion rate was >96% (Supplementary Table 4). Bisulphite-modified DNA was subjected to duplex-nested PCR.

Twenty-five (paternal alleles) or 26 (maternal alleles) CpG sites of the LYON-ES1, ORMES-1 and ORMES-6 monkey ESC lines in a 324 bp fragment of the *SNRPN* DMR (126678–127001, NC_007864.1) harbouring a G/C SNP at nucleotide 126776 for LYON-ES1 or G/C and A/G at positions 126776 and 126951, respectively, for ORMES-1 or G/T at nucleotide 126954 for ORMES-6 and 25 CpG in a 427 bp fragment of *H19/IGF2* DMR (222-649; AY725988.1) harbouring a SNP T/A at nucleotide 252 for LYON-ES1 cells (Fig. 3A and D), or three SNPs A/G, G/A and A/G at positions 331, 335 and 336, respectively, for ORMES-1 or three SNPs CG/TA and CG at positions 417, 418 and 429, respectively, for ORMES-6.

For human ESC line H9, we analysed 21 CpG sites in a 326 bp fragment of *H19/IGF2* DMR (7771-8096; AF125183) harbouring a SNP T/A at nucleotide 8008. The following primers specific for bisulphite-converted DNA, and specific to the monkey and human sequences, were used:

monkey *SNRPN*,
external forward: 5′-GGTATGTTTATTGATTTTAGGTTGTTTATGG-3′
external reverse: 5′-AAATATCTAATAAATAAAAATAACTACTCCCCAAA-3′
internal forward: 5′-GTAATAATGTTGTGGGGTTTTAGGG-3′
internal reverse: 5′-CTAATAAATAAAAATAACTACTCCCCAAACTATCTC-3′;
monkey *H19/IGF2*,
external forward: 5′-GGTYGTGAGGGATAGGATATTTAT-3′
external reverse: 5′-AATATAACCCCACCTAAAAACCTAATAC-3′
internal forward: 5′-GGTYGTGAGGGATAGGATATTTAT-3′
internal reverse: 5′-CCCATAAATATCCTATTCCCAAAT-3′;
human *H19/IGF2*,
external forward: 5′-AATAATGAGGTGTTTTAGTTTTATGGATG-3′
external reverse: 5′-ACTTAAATCCCAAACCATAACACTAAAAC-3′
internal forward 5′-AATAATGAGGTGTTTTAGTTTTATGGATG-3′
internal reverse 5′-ATAAATATCCTATTCCCAAATAACCCC 3′

The PCR products were subcloned into the pGEM-T plasmid (Promega) and 20–40 clones were sequenced for each PCR product (Biofidal). In contrast to the pyrosequencing analysis, bisulphite sequencing combined with SNPs enables precise quantification of the DMR methylation rate at each allele. Each sequence was carefully examined, and identical alleles were counted only once. The presence of uncertain, modified or deleted nucleotides (<3%; Supplementary Table 4) enabled us to discriminate distinct alleles that showed apparently identical methylation profiles. The bisulphite sequencing protocol was validated using genomic DNA extracted from the blood of the female who provided the oocytes to derive the LYON-ES1 cells. Mean *H19/IGF2* DMR methylation rate was $56 \pm 2\%$, indicating no bias toward methylated or non-methylated alleles. This DMR was highly methylated ($94.0 \pm 0.3\%$) in sperm, as expected. A statistical analysis of methylation rates was carried out using analysis of variance, and differences were considered significant when $p < 0.05$. We used Fisher's exact test to determine allele methylation status.

Supplementary data to this article can be found online at http://dx.doi.org/10.1016/j.scr.2016.03.002.

Author contributions

FW conceived the study, performed the experiments and wrote the manuscript; TB, CV and RG performed the experiments; MG analysed data and revised the manuscript; AL helped conceive, design and obtain financial support for the study; PYB and PS interpreted the data and revised the manuscript and CD conceived the study, revised the manuscript and obtained the funding.

Competing financial interests

The authors declare no competing financial interests.

Acknowledgements

We are indebted to P. Giroud for technical assistance. We thank Irène Aksoy for providing the Q-PCR primers, John DeVos for providing genomic DNA and total RNA of the HS306 human ESC line, and Shoukhrat Mitalipov for providing the monkey ORMES1 and ORMES6 ESC lines. This study was supported by Agence de Biomédecine « Recherche et Greffe » 2010; Fondation de l'Avenir (project N°ET2-645); FRM-Prix Victor et Erminia Mescle 2012 (project N°PME20120624812), LABEX CORTEX (ANR-11-LABX-0042), and LABEX DEVweCAN (ANR-10-LABX-061) of Université de Lyon, within the programme 'Investissements d'Avenir' (ANR-11-IDEX-0007) operated by the French National Research Agency (ANR); IHU CESAME (ANR-10-IBHU-0003).

References

Adewumi, O., et al., 2007. Characterization of human embryonic stem cell lines by the international stem cell initiative. Nat. Biotechnol. 25, 803–816.
Al-Khtib, M., et al., 2011. Vitrification at the germinal vesicle stage does not affect the methylation profile of H19 and KCNQ1OT1 imprinting centers in human oocytes subsequently matured in vitro. Fertil. Steril. 95, 1955–1960.
Allegrucci, C., et al., 2007. Restriction landmark genome scanning identifies culture-induced DNA methylation instability in the human embryonic stem cell epigenome. Hum. Mol. Genet. 16, 1253–1268.
Baharvand, H., et al., 2006. Generation of new human embryonic stem cell lines with diploid and triploid karyotypes. Develop. Growth Differ. 48, 117–128.
Borghol, N., Lornage, J., Blachere, T., Sophie Garret, A., Lefevre, A., 2006. Epigenetic status of the H19 locus in human oocytes following in vitro maturation. Genomics 87, 417–426.
Bowdin, S., et al., 2007. A survey of assisted reproductive technology births and imprinting disorders. Hum. Reprod. 22, 3237–3240.
Brioude, F., et al., 2013. Beckwith–Wiedemann syndrome: growth pattern and tumor risk according to molecular mechanism, and guidelines for tumor surveillance. Horm. Res. Paediatr. 80, 457–465.
Buiting, K., et al., 1995. Inherited microdeletions in the Angelman and Prader–Willi syndromes define an imprinting centre on human chromosome 15. Nat. Genet. 9, 395–400.
Chen, T., Ueda, Y., Dodge, J.E., Wang, Z., Li, E., 2003. Establishment and maintenance of genomic methylation patterns in mouse embryonic stem cells by Dnmt3a and Dnmt3b. Mol. Cell. Biol. 23, 5594–5605.
Chen, S.L., Shi, X.Y., Zheng, H.Y., Wu, F.R., Luo, C., 2010. Aberrant DNA methylation of imprinted H19 gene in human preimplantation embryos. Fertil. Steril. 94 (2356–2358, 2358 e2351).
Chen, H., et al., 2015. Reinforcement of STAT3 activity reprogrammes human embryonic stem cells to naive-like pluripotency. Nat. Commun. 6, 7095.
DeBaun, M.R., Niemitz, E.L., Feinberg, A.P., 2003. Association of in vitro fertilization with Beckwith–Wiedemann syndrome and epigenetic alterations of LIT1 and H19. Am. J. Hum. Genet. 72, 156–160.
Demars, J., Gicquel, C., 2012. Epigenetic and genetic disturbance of the imprinted 11p15 region in Beckwith–Wiedemann and Silver–Russell syndromes. Clin. Genet. 81, 350–361.
Doherty, A.S., Mann, M.R., Tremblay, K.D., Bartolomei, M.S., Schultz, R.M., 2000. Differential effects of culture on imprinted H19 expression in the preimplantation mouse embryo. Biol. Reprod. 62, 1526–1535.
Feinberg, A.P., 2004. The epigenetics of cancer etiology. Semin. Cancer Biol. 14, 427–432.
Fluckiger, A.C., et al., 2006. Cell cycle features of primate embryonic stem cells. Stem Cells 24, 547–556.
Frost, J., et al., 2011. The effects of culture on genomic imprinting profiles in human embryonic and fetal mesenchymal stem cells. Epigenetics 6, 52–62.

Fujimoto, A., Mitalipov, S.M., Kuo, H.C., Wolf, D.P., 2006. Aberrant genomic imprinting in rhesus monkey embryonic stem cells. Stem Cells 24, 595–603.
Gicquel, C., et al., 2003. In vitro fertilization may increase the risk of Beckwith–Wiedemann syndrome related to the abnormal imprinting of the KCN1OT gene. Am. J. Hum. Genet. 72, 1338–1341.
Gicquel, C., et al., 2005. Epimutation of the telomeric imprinting center region on chromosome 11p15 in Silver–Russell syndrome. Nat. Genet. 37, 1003–1007.
Grace, K.S., Sinclair, K.D., 2009. Assisted reproductive technology, epigenetics, and long-term health: a developmental time bomb still ticking. Semin. Reprod. Med. 27, 409–416.
Grybek, V., et al., 2014. Methylation and transcripts expression at the imprinted GNAS locus in human embryonic and induced pluripotent stem cells and their derivatives. Stem Cell Rep. 3, 432–443.
Hajkova, P., et al., 2002. Epigenetic reprogramming in mouse primordial germ cells. Mech. Dev. 117, 15–23.
Humpherys, D., et al., 2001. Epigenetic instability in ES cells and cloned mice. Science 293, 95–97.
Ibala-Romdhane, S., et al., 2011. Analysis of H19 methylation in control and abnormal human embryos, sperm and oocytes. Eur. J. Hum. Genet. 19, 1138–1143.
Inzunza, J., et al., 2005. Derivation of human embryonic stem cell lines in serum replacement medium using postnatal human fibroblasts as feeder cells. Stem Cells 23, 544–549.
Joo, J.Y., et al., 2014. Establishment of a primed pluripotent epiblast stem cell in FGF4-based conditions. Sci. Report. 4, 7477.
Keniry, A., et al., 2012. The H19 lincRNA is a developmental reservoir of miR-675 that suppresses growth and Igf1r. Nat. Cell Biol. 14, 659–665.
Khosla, S., Dean, W., Brown, D., Reik, W., Feil, R., 2001. Culture of preimplantation mouse embryos affects fetal development and the expression of imprinted genes. Biol. Reprod. 64, 918–926.
Khoueiry, R., et al., 2008. Dynamic CpG methylation of the KCNQ1OT1 gene during maturation of human oocytes. J. Med. Genet. 45, 583–588.
Khoueiry, R., et al., 2013. Abnormal methylation of KCNQ1OT1 and differential methylation of H19 imprinting control regions in human ICSI embryos. Zygote 21, 129–138.
Kim, K.P., et al., 2007a. Gene-specific vulnerability to imprinting variability in human embryonic stem cell lines. Genome Res. 17, 1731–1742.
Kim, J., Bergmann, A., Choo, J.H., Stubbs, L., 2007b. Genomic organization and imprinting of the Peg3 domain in bovine. Genomics 90, 85–92.
Lee, J.E., Pintar, J., Efstratiadis, A., 1990. Pattern of the insulin-like growth factor II gene expression during early mouse embryogenesis. Development 110, 151–159.
Lefevre, A., Blachere, T., 2015. Methylation of specific regions: bisulfite-sequencing at the single oocyte or 2-cell embryo level. Methods Mol. Biol. 1222, 209–226.
Leff, S.E., et al., 1992. Maternal imprinting of the mouse Snrpn gene and conserved linkage homology with the human Prader–Willi syndrome region. Nat. Genet. 2, 259–264.
Liao, J., et al., 2015. Targeted disruption of DNMT1, DNMT3A and DNMT3B in human embryonic stem cells. Nat. Genet. 47, 469–478.
Maher, E.R., et al., 2003. Beckwith-Wiedemann syndrome and assisted reproduction technology (ART). J. Med. Genet. 40, 62–64.
Mai, X., Mai, Q., Li, T., Zhou, C., 2011. Dynamic expression patterns of imprinted genes in human embryonic stem cells following prolonged passaging and differentiation. J. Assist. Reprod. Genet. 28, 315–323.
Mann, M.R., et al., 2004. Selective loss of imprinting in the placenta following preimplantation development in culture. Development 131, 3727–3735.
McCann, A.H., et al., 1996. Biallelic expression of the IGF2 gene in human breast disease. Hum. Mol. Genet. 5, 1123–1127.
Mitalipov, S.M., 2006. Genomic imprinting in primate embryos and embryonic stem cells. Reprod. Fertil. Dev. 18, 817–821.
Mitalipov, S., et al., 2006. Isolation and characterization of novel rhesus monkey embryonic stem cell lines. Stem Cells 24, 2177–2186.
Mitalipov, S., Clepper, L., Sritanaudomchai, H., Fujimoto, A., Wolf, D., 2007. Methylation status of imprinting centers for H19/IGF2 and SNURF/SNRPN in primate embryonic stem cells. Stem Cells 25, 581–588.
Mitalipova, M., et al., 2003. Human embryonic stem cell lines derived from discarded embryos. Stem Cells 21, 521–526.
Nazor, K.L., et al., 2012. Recurrent variations in DNA methylation in human pluripotent stem cells and their differentiated derivatives. Cell Stem Cell 10, 620–634.
Negron-Perez, V.M., Echevarria, F.D., Huffman, S.R., Rivera, R.M., 2013. Determination of allelic expression of h19 in pre- and peri-implantation mouse embryos. Biol. Reprod. 88, 97.
Nissenbaum, J., Bar-Nur, O., Ben-David, E., Benvenisty, N., 2013. Global indiscriminate methylation in cell-specific gene promoters following reprogramming into human induced pluripotent stem cells. Stem Cell Rep. 1, 509–517.
Okano, M., Bell, D.W., Haber, D.A., Li, E., 1999. DNA methyltransferases Dnmt3a and Dnmt3b are essential for de novo methylation and mammalian development. Cell 99, 247–257.
O'Leary, T., et al., 2013. Derivation of human embryonic stem cells using a post-inner cell mass intermediate. Nat. Protoc. 8, 254–264.
Orstavik, K.H., 1999. Genomic imprinting and hereditary diseases]. *Tidsskrift for den Norske laegeforening: tidsskrift for praktisk medicin, ny raekke*. 119 pp. 835–838.
Orstavik, K.H., et al., 2003. Another case of imprinting defect in a girl with Angelman syndrome who was conceived by intracytoplasmic semen injection. Am. J. Hum. Genet. 72, 218–219.
Pickering, S.J., et al., 2003. Preimplantation genetic diagnosis as a novel source of embryos for stem cell research. Reprod. BioMed. Online 7, 353–364.
Ragina, N.P., et al., 2012. Downregulation of H19 improves the differentiation potential of mouse parthenogenetic embryonic stem cells. Stem Cells Dev. 21, 1134–1144.
Reed, M.L., Leff, S.E., 1994. Maternal imprinting of human SNRPN, a gene deleted in Prader–Willi syndrome. Nat. Genet. 6, 163–167.
Reik, W., Walter, J., 2001. Genomic imprinting: parental influence on the genome. Nat. Rev. Genet. 2, 21–32.
Rugg-Gunn, P.J., Ferguson-Smith, A.C., Pedersen, R.A., 2005. Epigenetic status of human embryonic stem cells. Nat. Genet. 37, 585–587.
Rugg-Gunn, P.J., Ferguson-Smith, A.C., Pedersen, R.A., 2007. Status of genomic imprinting in human embryonic stem cells as revealed by a large cohort of independently derived and maintained lines. Hum. Mol. Genet. R243–R251 16 Spec No. 2.
Sasaki, H., Ferguson-Smith, A.C., Shum, A.S., Barton, S.C., Surani, M.A., 1995. Temporal and spatial regulation of H19 imprinting in normal and uniparental mouse embryos. Development 121, 4195–4202.
Sasaki, E., et al., 2005. Establishment of novel embryonic stem cell lines derived from the common marmoset (*Callithrix jacchus*). Stem Cells 23, 1304–1313.
Schumacher, A., Doerfler, W., 2004. Influence of in vitro manipulation on the stability of methylation patterns in the Snurf/Snrpn-imprinting region in mouse embryonic stem cells. Nucleic Acids Res. 32, 1566–1576.
Sperger, J.M., et al., 2003. Gene expression patterns in human embryonic stem cells and human pluripotent germ cell tumors. Proc. Natl. Acad. Sci. U. S. A. 100, 13350–13355.
Stadtfeld, M., et al., 2010. Aberrant silencing of imprinted genes on chromosome 12qF1 in mouse induced pluripotent stem cells. Nature 465, 175–181.
Sun, B.W., et al., 2006. Temporal and parental-specific expression of imprinted genes in a newly derived Chinese human embryonic stem cell line and embryoid bodies. Hum. Mol. Genet. 15, 65–75.
Sun, B., et al., 2012. Status of genomic imprinting in epigenetically distinct pluripotent stem cells. Stem Cells 30, 161–168.
Takai, D., Gonzales, F.A., Tsai, Y.C., Thayer, M.J., Jones, P.A., 2001. Large scale mapping of methylcytosines in CTCF-binding sites in the human H19 promoter and aberrant hypomethylation in human bladder cancer. Hum. Mol. Genet. 10, 2619–2626.
Tang, F., et al., 2010. Tracing the derivation of embryonic stem cells from the inner cell mass by single-cell RNA-Seq analysis. Cell Stem Cell 6, 468–478.
Thomson, J.A., et al., 1998. Embryonic stem cell lines derived from human blastocysts. Science 282, 1145–1147.
Watanabe, D., Suetake, I., Tada, T., Tajima, S., 2002. Stage- and cell-specific expression of Dnmt3a and Dnmt3b during embryogenesis. Mech. Dev. 118, 187–190.
Weksberg, R., Smith, A.C., Squire, J., Sadowski, P., 2003. Beckwith–Wiedemann syndrome demonstrates a role for epigenetic control of normal development. Hum. Mol. Genet. R61–R68 12 Spec No 1.
Wianny, F., et al., 2008. Derivation and cloning of a novel rhesus embryonic stem cell line stably expressing tau-green fluorescent protein. Stem Cells 26, 1444–1453.
Zhang, Y., et al., 1993. Imprinting of human H19: allele-specific CpG methylation, loss of the active allele in Wilms tumor, and potential for somatic allele switching. Am. J. Hum. Genet. 53, 113–124.